

# 9. Variational Monte Carlo Techniques in Nuclear Physics

*J.A. Carlson and R.B. Wiringa*

## 9.1 Introduction

Variational Monte Carlo techniques have proven to be a very powerful tool for studying quantum systems in the physics community as a whole, and particularly within nuclear physics [9.1–4]. The most important applications in nuclear physics are to few-body systems, either at the nucleon or the quark level. A variety of nuclear properties have been calculated with Monte Carlo methods, including the binding energies, electromagnetic form factors, response functions, and asymptotic properties of the wave functions for three- and four-body nuclei. One can also study the Hamiltonian itself, in particular the effects of three-nucleon interactions in light nuclei. Finally, one can examine low-energy scattering states and electromagnetic and weak transitions with these same methods.

One can also employ variational Monte Carlo methods to study the hadronic spectra in a variety of quark models. The flux-tube model, in particular, has been studied extensively with this method [9.5,6]. In addition to the baryon spectra, one can study the decays of these states, and also the spectra of so-called “exotic” four- and six-quark states. Although we will not cover this subject in any detail here, the computational principles involved are exactly the same as those used to study light nuclei. The major differences are simply in the basis of states employed, and, of course, in the interactions used to model these systems.

Two ingredients are necessary to perform any meaningful variational calculation. The first is good physical insight into the structure of the system. Variational studies are always limited by the form chosen for the wave function, and consequently care must be taken when drawing conclusions based upon its detailed properties. Although it may be easy to estimate the statistical error arising from a Monte Carlo calculation, it is much more difficult to determine the sensitivity to the parametrization.

Given an accurate form for the trial wave function, one must still be able to evaluate the integrals with sufficient accuracy to perform a variational calculation. This problem is far from trivial, especially in the context of nuclear physics, where the interactions are highly state-dependent. A great deal of work has been done on  $A = 3$  and  $4$  nuclei, including studies of the three-nucleon interaction and electromagnetic form factors. In addition, the  $A = 5$  problem [9.7] has been studied with simple generalizations of the variational Monte Carlo algorithms presented in this chapter. These methods should allow one to treat nuclei up to  $A = 8$ , and also to study light hypernuclei with realistic hyperon–nucleon interaction models. Investigations in

both of these areas are currently underway.

In addition, variational wave functions of the same form are believed to accurately describe the properties of heavier nuclei. Cluster expansion techniques [9.8] have recently been developed which should allow one to study heavier nuclei such as  $^{16}\text{O}$ .

The ground states of light nuclei have also been studied with Green's function Monte Carlo (GFMC) methods, which are very similar to the variational techniques described here. GFMC solves for the ground state of a quantum system by calculating

$$\Psi_0 = \exp\{-H\tau\}\Psi_T, \quad (9.1)$$

where  $\Psi_T$  is the variational wave function,  $\Psi_0$  is the exact ground state, and  $\tau$  is sufficiently large to project out all excited states. Various formulations of this method are described in some detail in Refs. [9.9–12], and its specific application to nuclear physics problems in Refs. [9.13,14].

## 9.2 General Methods

All variational Monte Carlo calculations rely upon a few simple ideas which we can describe only briefly. The interested reader is invited to consult Refs. [9.15,16] for examples of variational calculations in other areas of physics. Nearly all of these calculations rely upon the Metropolis algorithm [9.17] for generating a set of points with a specific probability distribution. This technique, as well as many other important general Monte Carlo topics, are covered in Ref. [9.18].

To study the ground state of a quantum system, one can make an ansatz for the wave function  $\Psi\{\alpha\}$ , where  $\{\alpha\}$  represents a set of variational parameters that are to be optimized. The expectation value of the Hamiltonian with this wave function gives an estimate of the ground-state energy

$$E\{\alpha\} = \frac{\langle\Psi|H|\Psi\rangle}{\langle\Psi|\Psi\rangle}, \quad (9.2)$$

where  $E\{\alpha\}$  is greater than the true ground-state energy  $E_0$ . By minimizing  $E\{\alpha\}$  with respect to each of the parameters, one obtains an approximation to both  $E_0$  and the ground-state wave function. The error in the estimated ground-state energy is second order in the difference between the trial and true ground-state wave functions, so it is often quite accurate. Expectation values of other observables, however, do not share this property.

It has occasionally proven useful to minimize other quantities, for example the difference

$$\langle H^2 \rangle - \langle H \rangle^2. \quad (9.3)$$

This difference is precisely zero for any true eigenstate of the Hamiltonian, so that in principle it can also be used to determine the excited states, assuming that one has a sufficiently accurate starting trial function. This technique also can be useful for choosing optimum trial wave functions for Green's function Monte Carlo calculations.

Variational Monte Carlo calculations determine  $E\{\alpha\}$  by writing it as

$$\langle H \rangle = \frac{\int d\mathbf{R} \frac{\Psi^\dagger(\mathbf{R}) H \Psi(\mathbf{R})}{W(\mathbf{R})} W(\mathbf{R})}{\int d\mathbf{R} \frac{\Psi^\dagger(\mathbf{R}) \Psi(\mathbf{R})}{W(\mathbf{R})} W(\mathbf{R})}. \quad (9.4)$$

$W(\mathbf{R})$  is a probability distribution usually taken to be just  $\Psi^\dagger(\mathbf{R})\Psi(\mathbf{R})$ . The value of this expression is that it can be easily evaluated through Metropolis Monte Carlo techniques, which can produce a set of points in the  $3A$ -dimensional space proportional to  $W(\mathbf{R})$ . Once this set of points  $\{\mathbf{R}\}$  is obtained, the expectation value of an operator  $O$  may be calculated through:

$$\langle O \rangle = \frac{\sum \frac{\Psi^\dagger(\mathbf{R}) O \Psi(\mathbf{R})}{W(\mathbf{R})}}{\sum \frac{\Psi^\dagger(\mathbf{R}) \Psi(\mathbf{R})}{W(\mathbf{R})}}, \quad (9.5)$$

where the sum runs over all the points in the set  $\{\mathbf{R}\}$ . This method is sufficient, in principle, to determine the expectation value of any operator  $O$ . In practice, its effectiveness depends largely upon the structure of the operator. For example, the true wave function is an eigenstate of the Hamiltonian, so each point in the average over the set  $\{\mathbf{R}\}$  makes an equal contribution. Therefore, in the limit that the variational wave function approaches the exact eigenstate, there is no statistical error associated with Monte Carlo evaluations of  $\langle H \rangle$ .

In reality, of course, there is always a statistical error, since we do not know the exact wave function. This error can be estimated by making use of the central limit theorem. If there are a sufficiently large number of statistically independent samples in the set  $\{\mathbf{R}\}$ , the distribution of "local" averages obtained in a Monte Carlo evaluation is simply a Gaussian centered on the true value. A "local" average is simply the average over a sufficiently large set of the points in  $\{\mathbf{R}\}$ , and thus the distribution of local averages obtained during a simulation can be used to estimate the statistical error of the calculation:

$$\sigma = \sqrt{\frac{\langle O^2 \rangle - \langle O \rangle^2}{N - 1}}, \quad (9.6)$$

where  $N$  is the number of local averages, and  $\sigma$  represents a one-standard-deviation error estimate. Authentic two-standard-deviation effects will occur approximately in one out of twenty calculations.

Great care must be taken to ensure that these local averages are indeed statistically independent and also that any dependence on initial conditions has disappeared. Apparently two-standard-deviation effects appear very often in the literature, often owing to neglect of the terms "sufficiently large" and "statistically independent". These phrases are meaningful only in the context of a specific problem, and their precise values must be determined by experiment in each new calculation. They also depend strongly upon the operator of interest, and not simply on the ground-state wave function. Other error-analysis methods, such as "bootstrapping", are available in cases where the statistical results are more limited. These techniques can be very useful, and they do not rely upon a Gaussian distribution of statistical errors. In general, though, they are unnecessary for analyzing results in light nuclei.

Metropolis Monte Carlo algorithms generate a set of points  $\mathbf{R}$  with probability distribution  $W(\mathbf{R})$  through the following basic algorithm:

1. Given a  $3A$ -dimensional vector  $\mathbf{R}$ , generate a new vector  $\mathbf{R}'$  with a "transition probability"  $T(\mathbf{R} \Rightarrow \mathbf{R}')$ . In the simplest case,  $T$  is taken to be a constant within a  $3A$ -dimensional cube surrounding the point  $\mathbf{R}$ .
2. Calculate the quantities  $W(\mathbf{R})$ ,  $W(\mathbf{R}')$ ,  $T(\mathbf{R} \Rightarrow \mathbf{R}')$ , and  $T(\mathbf{R}' \Rightarrow \mathbf{R})$ , the transition probability for the reverse step. The acceptance probability is given by the expression

$$P(\mathbf{R} \Rightarrow \mathbf{R}') = \min\{1, W(\mathbf{R}')T(\mathbf{R}' \Rightarrow \mathbf{R})/W(\mathbf{R})T(\mathbf{R} \Rightarrow \mathbf{R}')\}.(9.7)$$

3. If the move is accepted, set  $\mathbf{R} = \mathbf{R}'$  and return to step one. Otherwise, discard the point  $\mathbf{R}'$  and generate the next move from the original  $\mathbf{R}$ .

This algorithm satisfies the condition known as "detailed balance"; that is, that the combined probability for a move from  $\mathbf{R}$  to  $\mathbf{R}'$  is equal to the probability for the reverse move. By combined probability one means the product of the probability of being at  $\mathbf{R}$  to begin with, which we want to be  $W(\mathbf{R})$ , the probability for trying a move from  $\mathbf{R}$  to  $\mathbf{R}'$ ,  $T(\mathbf{R} \Rightarrow \mathbf{R}')$ , and the probability for accepting such a move  $P(\mathbf{R} \Rightarrow \mathbf{R}')$ . It is trivial to show that the definition of  $P$  given in step 2 satisfies this condition.

One must be careful, of course, to use only those points generated after the equilibrium distribution has been reached. This can be determined by tracking various expectation values as a function of the number of Monte Carlo steps. For the simple few-body problems considered here, the equilibrium distribution is usually reached fairly rapidly (a few hundred steps),

and for most operators statistically independent samples will be obtained within at most a similar number of steps.

Instead of using a constant (within a prescribed volume  $V$ ) for the transition probability  $T$ , one can use information about the derivatives of  $W$  to obtain a more efficient sampling of configuration space. For a given volume  $V$ , these “forced bias” [9.18] algorithms give, on average, a higher acceptance probability  $P$ . One need only take care that  $P(\mathbf{R} \Rightarrow \mathbf{R}')$  is never less than zero for any  $\mathbf{R}$  and  $\mathbf{R}'$ . The step size used in the algorithm should be adjusted to minimize the computer time necessary to generate statistically independent results. The lore in this field holds that an acceptance ratio of roughly fifty percent usually gives good results.

Finally, one can often use so-called “expected-value” [9.18] methods to reduce the variance of a calculation. Instead of simply averaging over the set of points  $\mathbf{R}$  reached in step 1 of the algorithm, one can average at each step  $P$  times the value at point  $\mathbf{R}'$  with  $(1 - P)$  times the value at the old point  $\mathbf{R}$ . This, of course, gives the same contribution on average to the integral in question. This technique is primarily useful when the quantity of interest is rather cheap to compute compared to the evaluation of  $W$  (here the square of the wave function).

### 9.3 Interactions and Wave Functions

Realistic treatments of problems in nuclear physics typically involve highly state-dependent interactions. When studying hadron spectra, one is dealing with operators based upon “one-gluon-exchange” interactions [9.19]. We will concentrate on few-nucleon problems, for which the Hamiltonian may be written as

$$H = \sum_i \frac{-\hbar^2}{2m} \nabla_i^2 + \sum_{i < j} \sum_k V^k(r_{ij}) O_{ij}^k + \sum_{i < j < k} V_{ijk}. \quad (9.8)$$

The operators  $O_{ij}^k$  in realistic nucleon–nucleon interactions (Argonne  $v_{14}$  [9.20], Paris [9.21], Nijmegen [9.22], Reid [9.23], etc.) may be taken to be

$$O_{ij}^k = [1, \sigma_i \cdot \sigma_j, S_{ij}, (L \cdot S)_{ij}, L_{ij}^2, L_{ij}^2 \sigma_i \cdot \sigma_j, \nabla_{ij}^2, \nabla_{ij}^2 \sigma_i \cdot \sigma_j, (L \cdot S)_{ij}^2] \\ \otimes [1, \tau_i \cdot \tau_j]. \quad (9.9)$$

These interactions are generally fit to nucleon–nucleon scattering data and deuteron properties, and include the one-pion-exchange interaction at long distances. At intermediate and short distances, they are more phenomenological, often assuming a one-boson-exchange structure.

There are significant differences between the various interaction models; for instance the D-state of the deuteron ranges from 5.2% to 6.5%. We cannot describe the individual models in detail, but we note that the same

methods can be applied to each of the interactions. The three-body interactions are expected to be of some importance in nuclear physics, simply because the energy scale for internal excitations of the nucleon is fairly small (hundreds of MeV). Various models for the three-nucleon interactions have been proposed [9.2,24]; these models incorporate the operator structure of the two-pion-exchange-three-nucleon interaction at long distances.

The variational wave functions employed to study these Hamiltonians have the following general structure:

$$\Psi = \left( S \prod_{i < j} F_{ij} \right) \Phi. \quad (9.10)$$

The  $F_{ij}$  are pair-correlation operators and  $\Phi$  is an antisymmetrized product of one-body states. The  $F_{ij}$  are generally noncommuting so the product must be symmetrized. The combination of strong short-ranged repulsion and strong state dependence in the interaction makes this a good choice for the trial function. The product of one-body states  $\Phi$  incorporates the correct total angular momentum and isospin for the state of interest. We can also choose it to be independent of the center of mass in order to insure the translational invariance of the full wave function. For three- and four-body nuclei  $\Phi$  is simply taken to be a product of spin-isospin states with no spatial dependence:

$$\Phi({}^3\text{He}) = \mathcal{A} | \uparrow n \downarrow p \uparrow p \rangle; \quad (9.11)$$

$$\Phi({}^4\text{He}) = \mathcal{A} | \uparrow n \downarrow n \uparrow p \downarrow p \rangle. \quad (9.12)$$

In this case, the correct asymptotic conditions on the wave function are imposed as conditions on the pair correlations. Of course, other choices are possible, and the choice of forms for  $\Phi$  and the pair correlations are closely related.

The pair correlations are chosen to reflect the influence of the two-body potential at short distances, while satisfying asymptotic boundary conditions of single-particle separability [9.3,4]. This is achieved by solving six Schrödinger-like equations in  $S, T$  channels: two single-channel equations for  $S = 0$  states, and two coupled-channel equations in the  $S = 1$  states. These equations give four central  $f_{S,T}$  and two tensor  $f_{t,T}$  functions that can then be projected into operator form. The six equations are the low-density limit of those used in nuclear matter studies [9.25] (without spin-orbit correlations):

$$\begin{aligned}
& - \frac{\hbar^2}{m} \left[ (f_{S,T} r^{l+1})'' - \frac{l(l+1)}{r^2} (f_{S,T} r^{l+1}) \right] \\
& + (\bar{v}_{S,T}\{\alpha\} + \lambda_{S,T})(f_{S,T} r^{l+1}) + 8(\bar{v}_{t,T}\{\alpha\} + \lambda_{t,T})(f_{t,T} r^{l+1})\delta_{S1} = 0,
\end{aligned} \tag{9.13}$$

and

$$\begin{aligned}
& - \frac{\hbar^2}{m} \left[ (f_{t,T} r^{l+1})'' - \frac{6+l(l+1)}{r^2} (f_{t,T} r^{l+1}) \right] \\
& + (\bar{v}_{S,T}\{\alpha\} + \lambda_{S,T} - 2(\bar{v}_{t,T}\{\alpha\} + \lambda_{t,T}) - 3\bar{v}_{b,T}\{\alpha\})(f_{t,T} r^{l+1}) \\
& + (\bar{v}_{t,T}\{\alpha\} + \lambda_{t,T})(f_{S,T} r^{l+1}) = 0,
\end{aligned} \tag{9.14}$$

where " denotes a second derivative, the  $\bar{v}\{\alpha\}$  are quenched potentials characterized by a variational parameter  $\alpha$  (including the spin-orbit potentials  $\bar{v}_{b,T}\{\alpha\}$ ), and  $l = 0(1)$  for  $S, T = 0, 1$  and  $1, 0$  ( 0, 0 and 1, 1 ). The boundary conditions for  $f_{S,T}$  and  $f_{t,T}$  are

$$\begin{aligned}
f_{S,T}(r \rightarrow 0) &= \text{constant} \\
f_{t,T}(r \rightarrow 0) &= 0 \\
f_{S,T}(r \rightarrow \infty) &= \left[ \frac{\exp(-k_{S,T} r)}{r} \right]^{1/(A-1)} \\
f_{t,T}(r \rightarrow \infty) &= \eta_T \left( 1 + \frac{3}{k_{S,T} r} + \frac{3}{(k_{S,T} r)^2} \right) \left[ \frac{\exp(-k_{S,T} r)}{r} \right]^{1/(A-1)},
\end{aligned} \tag{9.15}$$

with

$$k_{S,T} = \left[ \frac{A-1}{A} \frac{2m}{\hbar^2} E_{S,T} \right]^{1/2}. \tag{9.16}$$

The four separation energies  $E_{S,T}$  and two tensor/central ratios  $\eta_T$  are variational parameters. The Lagrange multipliers  $\lambda_x$  are radial functions consisting of two parts: the long-range part  $\Lambda_x(r)$  is fixed by the asymptotic behavior of  $f_x$  and is cut off at short distances by an exponential function, while the short-range part is a Woods-Saxon function multiplied by a constant  $\Gamma_x$ ;

$$\lambda_x = \Gamma_x \left[ 1 + \exp \left( \frac{r - R_x}{a_x} \right) \right]^{-1} + \Lambda_x(r) \{ 1 - \exp[-(r/c_x)^2] \}. \tag{9.17}$$

These constants are determined by solving the differential equations subject to the boundary conditions given above. The Woods-Saxon and cut-off constants ( $R_x$ ,  $a_x$ , and  $c_x$ ) are additional variational parameters. After solving the differential equations, the correlations are recast into operator form:

$$\sum_{\alpha} f_{\alpha}(r_{ij}) P_{ij}^{\alpha} = \sum_{k=1}^6 f^k(r_{ij}) O_{ij}^k = f^c(r_{ij}) \left[ 1 + \sum_{k=2}^6 u^k(r_{ij}) O_{ij}^k \right], \quad (9.18)$$

where the  $P^{\alpha}$  are channel projection operators and the operators  $O_{ij}^k$  are

$$O_{ij}^k = 1, \tau_i \cdot \tau_j, \sigma_i \cdot \sigma_j, \sigma_i \cdot \sigma_j \tau_i \cdot \tau_j, S_{ij}, S_{ij} \tau_i \cdot \tau_j. \quad (9.19)$$

Empirically it has been necessary to introduce three-body correlations which modify the strength of the two-body spin-dependent correlations whenever more than two particles are near each other. We have introduced a set of three-body correlations

$$f_3 = \prod_{k \neq i,j} \left[ 1 - t_1 \left( \frac{r_{ij}}{R} \right)^{t_2} \exp(-t_3 R) \right], \quad (9.20)$$

with  $R = r_{ij} + r_{ik} + r_{jk}$ . These correlations multiply the  $u^k$  in the equation above. The parameters  $t_1$ ,  $t_2$ , and  $t_3$  are determined variationally, and may in principle be different for each of the five correlation functions. In practice, we keep only two, one for the tensor operators and another for the nontensor terms.

## 9.4 Monte Carlo

Once we have defined a wave function and an interaction, we need to develop a code which will evaluate the expectation value of a strongly state-dependent Hamiltonian. This is fairly simple in principle, as we can rewrite (9.4) as

$$\langle H \rangle = \frac{\int d\mathbf{R} \sum_{kl} \frac{\Psi_k^{\dagger}(\mathbf{R}) \mathbf{H}_{kl} \Psi_l(\mathbf{R})}{W(\mathbf{R})} W(\mathbf{R})}{\int d\mathbf{R} \sum_{kl} \frac{\Psi_k^{\dagger}(\mathbf{R}) \Psi_l(\mathbf{R})}{W(\mathbf{R})} W(\mathbf{R})}, \quad (9.21)$$

where the sums over  $k$  and  $l$  run over all spin-isospin states. In principle, one could define a weight which is a function of  $k$  and  $l$ , and use Monte Carlo to evaluate these sums as well as the integrals in configuration space. However, this method will produce large statistical errors, because one is no longer making use of the cancellations that arise because the wave function is an eigenstate of the Hamiltonian. By performing the sums over spin and isospin states explicitly at each point in the walk rather than using Monte Carlo, the variance of the calculation can be greatly reduced. This explicit summation, though, limits the applicability of the algorithm to light ( $A \leq 8$ ) nuclei.

The form of variational wave function (9.10) implies the possibility of a further gain in efficiency. The symmetrization operator  $S$  indicates a sum over all orders of the pair correlation operators. For example,

$$S(F_{12}F_{13}F_{23}) = \frac{1}{\sqrt{6}}[F_{12}F_{13}F_{23} + F_{13}F_{12}F_{23} + F_{23}F_{12}F_{13} + \dots]. \quad (9.22)$$

Monte Carlo techniques can be used to sample the terms in the sum, choosing the order of operators independently for  $\Psi(\mathbf{R})$  and  $\Psi^\dagger(\mathbf{R})$ :

$$\begin{aligned}\Psi^\dagger(\mathbf{R}) &= \sum_p \Psi_p^\dagger(\mathbf{R}), \\ \Psi(\mathbf{R}) &= \sum_q \Psi_q(\mathbf{R}).\end{aligned}\quad (9.23)$$

In addition, the weight function  $W$  can be made a function of  $p$  and  $q$ . We have chosen

$$W_{pq}(\mathbf{R}) = |\text{Re}\langle \Psi_p^\dagger(\mathbf{R}) | \Psi_q(\mathbf{R}) \rangle|, \quad (9.24)$$

where the brackets indicate a sum over all spin and isospin states. The absolute magnitude is required in order to be certain that the weight function is never less than zero. In light nuclei, the real part of the product  $\langle \Psi_p^\dagger \Psi_q \rangle$  is positive for any  $p$  and  $q$  for reasonable choices of correlation functions.

The statistical error per sample in configuration space is increased by sampling the order of operators. However, the time saved by evaluating only one term in the sum increases the efficiency of the calculation, especially for  $A > 3$ . The complete expression for the expectation value of an operator  $O$  (analogous to (9.5)) is

$$\langle O \rangle = \frac{\frac{\langle \Psi_p^\dagger(\mathbf{R}) O \Psi_q(\mathbf{R}) \rangle}{W_{pq}(\mathbf{R})}}{\frac{\langle \Psi_p^\dagger(\mathbf{R}) \Psi_q(\mathbf{R}) \rangle}{W_{pq}(\mathbf{R})}}. \quad (9.25)$$

$W_{pq}(\mathbf{R})$  is the weight function used to generate the coordinates in configuration and permutation space, and the brackets indicate sums over all spin-isospin states.

It is often desirable to use a given set of configurations, obtained with one  $W_{pq}$ , to evaluate the energy of several different variational wave functions. Although this procedure produces a biased estimate of the energy (since both the numerator and denominator will contain a statistical error), it can be very valuable in minimizing the energy. There are often large cancellations in the difference in energy of two wave functions, and these cancellations can be exploited by using this “reweighting” technique. This method is most valuable for small changes in the wave function, in which case the bias is small. Once the variational parameters are optimized, one should always do a long unbiased run to produce the best estimate of the energy. In this manner one also eliminates another common problem with

variational Monte Carlo calculations: an artificial lowering of the energy estimate associated with using the same run to optimize the parameters and evaluate the energy.

A convenient basis of spin-isospin states is provided by those sets in which each particle has a definite third component of spin and isospin. The Hamiltonian and pair-correlation operators are sparse matrices in this basis, since two-body correlations or interactions can only change the spins or isospins of two nucleons at a time.

For example, the operator  $\sigma_i \cdot \sigma_j$  may be written as

$$\sigma_i \cdot \sigma_j = 2P_{ij}^\sigma - 1, \quad (9.26)$$

and the tensor operator

$$S_{ij} = 3(\sigma_i^+ \hat{r}^- + \sigma_i^- \hat{r}^+ + \sigma_i^0 \hat{r}^0)(\sigma_j^+ \hat{r}^- + \sigma_j^- \hat{r}^+ + \sigma_j^0 \hat{r}^0) - 2P_{ij}^\sigma + 1, \quad (9.27)$$

where

$$\begin{aligned} \sigma^+ &= (\sigma^x + i\sigma^y)/2 & \sigma^- &= (\sigma^x - i\sigma^y)/2 & \sigma^0 &= (\sigma^z), \\ \hat{r}^+ &= \hat{r}^x + i\hat{r}^y & \hat{r}^- &= \hat{r}^x - i\hat{r}^y & \hat{r}^0 &= \hat{r}^z, \end{aligned} \quad (9.28)$$

$P_{ij}^\sigma$  interchanges spins  $i$  and  $j$ , and  $\sigma^+$  and  $\sigma^-$  convert down spins to up and up to down, respectively.

Within the computer, it is convenient to represent the state  $\Psi_p$  as a two-dimensional complex array containing the coefficients associated with each spin-isospin state. The indices of the array represent, in a simple binary fashion, the spin and isospin states of the system. For example, the spin indices are given by

$$\begin{aligned} \downarrow\downarrow\downarrow\downarrow &= (0000)_{\text{base 2}} + 1 = 1 \\ \downarrow\downarrow\downarrow\uparrow &= (0001)_{\text{base 2}} + 1 = 2 \\ \downarrow\downarrow\uparrow\downarrow &= (0010)_{\text{base 2}} + 1 = 3 \\ \downarrow\downarrow\uparrow\uparrow &= (0011)_{\text{base 2}} + 1 = 4 \\ \uparrow\uparrow\uparrow\uparrow &= (1111)_{\text{base 2}} + 1 = 16. \end{aligned} \quad (9.29)$$

At this point, it is simple to create a table containing the results of acting with a spin-exchange operator for any pair acting on any initial state. Similarly, one can construct tables for the spin-flip ( $\sigma_i^+ + \sigma_i^-$ ) operator.

The isospin states are handled similarly, but not all bit patterns are retained because of charge conservation. Thus, there are only 6 isospin states in an alpha particle, but 16 spin states. One could further reduce the storage requirements by explicitly invoking isospin conservation, but this would necessitate a more complicated matrix structure for the isospin-exchange operator.

Once the operator tables are constructed, it is easy to compute the result of any operator of the form

$$O = \sum_{k=1}^6 c_k O_{ij}^k \quad (9.30)$$

acting on an arbitrary initial state. In this expression,  $c_k$  are complex coefficients and  $O^k$  are the six operators given in (9.19). One can easily compute the wave function  $\Psi_q$  by repeated operations of this sort, applying each pair operator consecutively. The expectation values of the static potential terms can be evaluated similarly.

The expectation value of the kinetic energy as well as other momentum-dependent terms in the interaction must also be evaluated. The kinetic energy and  $L \cdot S$  terms require both the first derivatives of the wave function and the diagonal second derivatives to be computed. These are obtained simply by moving each particle a small distance  $\epsilon$  in both the positive and negative directions along each axis:

$$\begin{aligned} \nabla_j^i \Psi\{\mathbf{R}\} &= [\Psi\{\mathbf{R} + \epsilon \hat{r}_j^i\} - \Psi\{\mathbf{R} - \epsilon \hat{r}_j^i\}]/[2\epsilon] \\ \nabla_j^{i^2} \Psi\{\mathbf{R}\} &= [\Psi\{\mathbf{R} + \epsilon \hat{r}_j^i\} + \Psi\{\mathbf{R} - \epsilon \hat{r}_j^i\}] - 2\Psi\{\mathbf{R}\}/[\epsilon^2]. \end{aligned} \quad (9.31)$$

In these expressions,  $i$  represents a direction ( $x, y$ , or  $z$ ), and  $j$  represents the particle. The  $L \cdot S$  operator can be rewritten in terms of  $\sigma^+, \sigma^-,$  and  $\sigma^0,$  as was done above for the tensor operator. In the interests of brevity, the program included with this chapter does not treat  $L^2$  or  $(L \cdot S)^2$  operators, and so is limited to simpler interaction models such as the Reid  $v_8$ , which is a simplification of the full Reid interaction [9.23]. The operators which contain two derivatives may be included either by using integration by parts to apply one derivative operator to  $\Psi(\mathbf{R})$  and one to  $\Psi^\dagger(\mathbf{R}),$  or by direct numerical calculation of the remaining second partial derivatives. This latter technique is necessary when trying to compute energy-weighted sum rules [9.26].

## 9.5 Results

The optimized variational parameters we have obtained for the triton with the Reid  $v_8$  interaction are listed in Table 9.1. These parameters were determined after a series of runs, many of which employed the reweighting techniques described above. Typically, twenty to thirty runs of several thousand configurations are necessary to optimize the parameters for each new interaction model. With reweighting techniques, it is fairly easy to evaluate the difference in energy between two similar wave functions to within a few hundredths of an MeV.

Once the optimum wave function has been determined, a set of Monte Carlo calculations should be undertaken to determine all of the expectation values. For the three-body problem, ten to twenty thousand configurations seem to provide reasonable statistical accuracy for the energy and one-body densities. Ten thousand configurations take roughly 30 minutes of CPU

**Table 9.1.** Triton Variational Parameters

	$^1S_0$	$^1P_1$	$^3S_1$	$^3P_J$	$^3D_1$	$^3F_J$
$E_{S,T}$	6.0	2.0	12.0	6.0	.026	-.010
$\eta_T$						
$c_x$	1.0	1.0	3.0	3.0	2.0	2.0
$a_x$	0.4	0.4	0.4	0.4	0.4	0.4
$R_x$	1.0	1.0	2.8	2.8	3.6	3.6
$\alpha_x$	1.00	0.92	0.92	0.92	0.92	0.92
	$t1_{S,T}$	$t1_{t,T}$	$t2_{S,T}$	$t2_{t,T}$	$t3_{S,T}$	$t3_{t,T}$
	10.0	10.0	4.0	4.0	0.05	0.05

time on a one megaflop computer. Of course, this calculation can be split up into many small runs, and the energies and statistical error determined from these results.

The results obtained with this wave function are summarized in Table 9.2 and Fig. 9.1. The table presents all of the energy expectation values, as well as point-particle rms radii of the neutron and proton density. In this table,  $V_{ij}$  gives the total nucleon–nucleon potential energy, and  $T_i$  is the total kinetic energy. There is a strong cancellation in the total energy owing to the strong repulsive core in the nucleon–nucleon interaction. The two-body potential is also split up into the  $V_6$  contribution and the remaining  $L \cdot S$  terms ( $V_b$ ).

**Table 9.2.** Triton Results

	Expectation Value	Statistical Error
$T_i + V_{ij}$	-7.30	0.04
$T_i + V_{ij} + V_{ijk}$	-8.44	0.06
$T_i$	52.4	0.6
$V_{ij}$	-59.7	0.6
$V_6$	-60.8	0.6
$V_b$	1.1	0.1
$V_{ijk}$	-1.14	0.03
$V3_a$	-1.04	0.02
$V3_c$	-0.68	0.02
$V3_u$	0.58	0.02
$\langle r_i^2 \rangle$ proton	1.620	0.004
$\langle r_i^2 \rangle$ neutron	1.766	0.004

In addition, the contribution of the various pieces of the Urbana model VII three-nucleon-interaction are given in Table 9.2. The commutator and

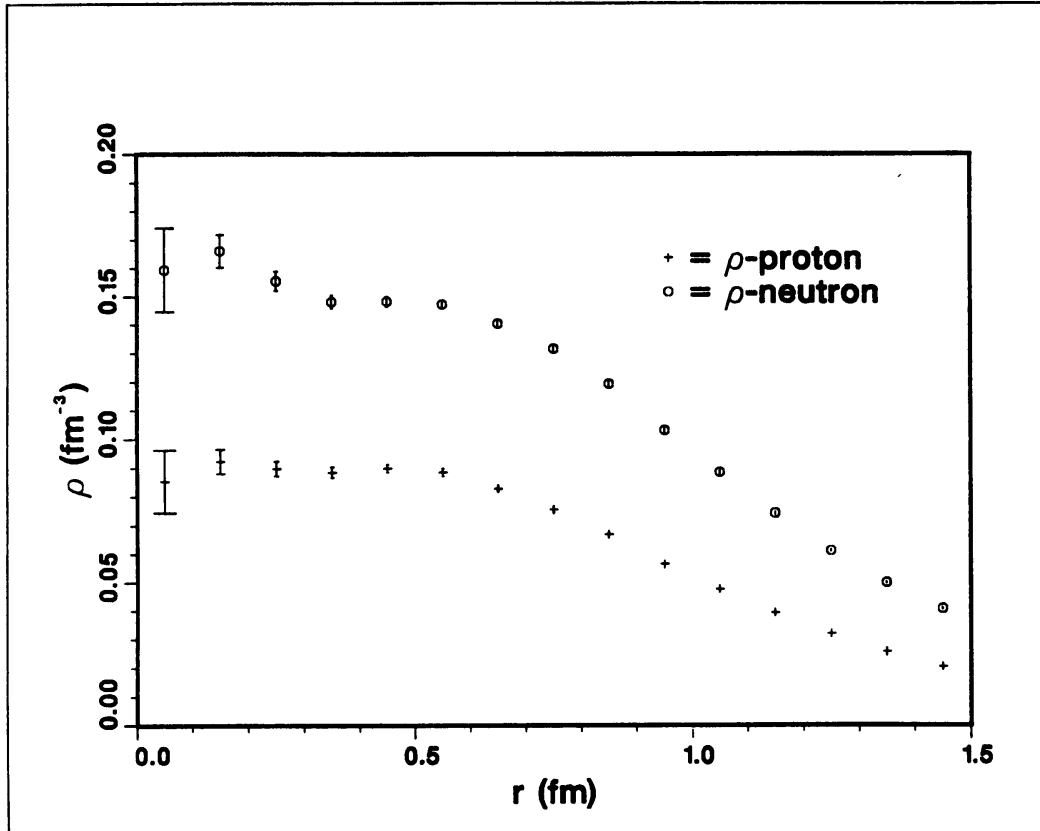


Fig. 9.1. Point proton and neutron densities in the triton for the Reid  $v_8 +$  Urbana VII TNI interaction.

anticommutator pieces of the two-pion-exchange TNI are listed as  $V3_c$  and  $V3_a$  respectively, and the short-ranged repulsive piece is  $V3_u$ . Each of these terms is a very small fraction of the total potential energy, yet they constitute a significant part of the binding energy of the three- and four-nucleon systems. The neutron and proton one-body densities are given in Fig. 9.1. The neutron and proton form factors can easily be folded in to get the charge density and then Fourier transformed to get the impulse approximation to the charge form factor. Meson exchange currents play a very important role in getting the correct charge form factor, even at relatively moderate values of the momentum transfer. The same Monte Carlo methods can be used to determine these expectation values. Schiavilla et al. have obtained excellent agreement with the charge form factors employing these methods [9.27].

Many other physically interesting quantities can be calculated, including non-energy-weighted [9.28] and energy-weighted Coulomb sum rules [9.26], momentum distributions, etc. The time required for any calculation depends not only upon the desired accuracy and the available computer capacity, but also on the operator one is interested in. The expectation values of nonlocal operators, for example the momentum distribution of nucleons in the nucleus, are particularly prone to high statistical error. In such

cases it is important to develop the best possible Monte Carlo algorithm to minimize the variance.

Taking a simple example, this code calculates the one-particle density as a function of the distance from the center of mass. The statistical errors in the density are quite large near the origin simply because of the  $r^2$  phase-space factor. If one is particularly interested in the density at this point, it would be very profitable to redo the calculation with a different weight function  $W$ , one which emphasizes configurations where at least one particle is near the center of mass.

Current work in light nuclei centers on the possibilities of treating larger systems and the dynamical properties of light nuclei. These methods hold promise in many avenues of nuclear physics. In particular, one can study parts of nuclear physics related to astrophysics, including neutron-rich nuclei and low-energy reactions. In addition, successful calculations of dynamical properties are extremely important to our understanding of current and future electron-scattering experiments.

## 9.6 Computer Code

The program presented here is a somewhat simplified version of our standard few-nucleon code. It contains one two-nucleon potential (Reid  $v_8$ ) and one three-nucleon potential (Urbana VII) and solves for the ground-state binding energy and density distribution for either three- or four-body nuclei. It can also save random walks generated with one trial function and then compute energy differences with a different trial function. It is written in ANSI standard FORTRAN 77 (with the exception of using lowercase letters) and we have verified that it runs on a number of different computers. The code includes performance monitoring, and benchmark information is presented in Table 9.3.

In the following, we describe the general structure of the code and point out some of the specific features. Details of the specific variables and actions of the program are given as comments in the code listing.

The computer code includes a main routine, called **NUCLEI**, and some 22 subroutines and functions. The code requires double-precision arithmetic and includes complex variables. Variables which specify the choice between the three- or four-body problems are set in **PARAMETER** statements that are shared by most of the program elements. (This improves efficiency by specifying many DO-loop lengths at compilation time.) A small data file is read in from unit **NIN** and output is sent to unit **NOUT**.

Initialization includes calls to a function **TIMER**, which starts timing data for monitoring performance, and a subroutine **HEADER**, which identifies the system, compiler, time, and date. These calls are machine specific; here we provide code (which is selected by removing appropriate comment prefixes in the subroutines) for the machines in Table 9.3. Data is read (and

**Table 9.3.** Code Performance and Timing. “Time” is the number of seconds required to compute one energy sample, including moving for a new walk. “Speed” is in MFLOPS.

Computer	Operating system / Fortran compiler	$^3\text{H}$ old walk		$^4\text{He}$ new walk	
		$T_i + V_{ij}$	time speed	$T_i + V_{ij} + V_{ijk}$	time speed
VAX 11/780	VMS / vax fortran v5.3	0.68	0.15	11.	0.15
Sun-3/160	UNIX / f77 -O -ffpa	0.48	0.21	8.7	0.20
VAX 3100	VMS / vax fortran v5.2	0.25	0.41	4.0	0.43
Sun-4/280	SunOS / f77 -O	0.13	0.80	2.0	0.88
VAX 8700	VMS / vax fortran v5.2	0.10	1.0	1.7	1.0
Sun Sparc 1	SunOS / f77 -O	0.10	1.0	1.7	1.1
IBM 3033	MVS / vs fortran 2.3.0	0.064	1.6	0.96	1.8
IBM 3090/VF	VM / vs fortran 2.3.0	0.030	3.3	0.34	5.1
Cray-2S	CTSS / cft77 3.1	0.0054	19.	0.050	37.
Cray X-MP	UNICOS / cft77 3.1.1.2	0.0037	28.	0.034	51.

printed) specifying the Hamiltonian. Potential functions are set by calls to subroutine POT.

Next, components of the wave function are initialized. The initial uncorrelated wave function  $\Phi$  of (9.11,12) and the spin-isospin matrices which give the result of spin-exchange and spin-flip operations on the wave function (9.26–28) are produced by subroutine SETSPN and its function EXCH. Data specifying the two-body correlation operator is read, and the correlation functions  $f^c$  and  $u^k$  are generated by the subroutine F6COR according to (9.14–18). An optional printout of the spin-isospin matrices and correlation functions is provided by subroutine WFPRT. Variables for the three-body correlation  $f_3$  of (9.20) are also read.

Variables controlling the random walk are read next. The pseudo-random-number generator is initialized with the call SETRND. The option of saving a random walk by writing a file on unit NRW, or of following a previously saved random walk by reading an existing file, is available. Additional variables are initialized, including the local and global energy sums. A starting wave function is then generated by following the general Metropolis moving procedure (provided by subroutine MOVEEM as discussed below) for a long enough time to randomize the particle positions and order of operators in the correlation-operator product. Alternatively, if a previous walk is being followed, subroutine REMOVE is used instead.

The calculation proceeds by obtaining a position  $\mathbf{R}$  drawn from the weight function  $W_{pq}(\mathbf{R})$  of (9.24). This is accomplished by a call to sub-

routine MOVEEM, which uses the Metropolis algorithm of (9.7). MOVEEM first uses the pseudo-random-number generator RNDNMB to select a new  $\mathbf{R}'$  and order of operators  $p'$  and  $q'$ . The use of our own pseudo-random-number generator ensures reproducibility of results when the code is moved from one machine to another. Pair distances and unit vectors are evaluated, and the corresponding functional values  $f^c$  and  $u^k$  are interpolated by subroutine INTERP. If any pair of particles is too close, or too far apart, for the three-point interpolation to be valid, the move is rejected and a warning counter is incremented. The  $\Psi_{p'}^\dagger(\mathbf{R}')$  and  $\Psi_{q'}(\mathbf{R}')$  are then constructed by calls to subroutine WAV.  $W_{p'q'}(\mathbf{R}')$  is calculated using the function RCDOT, which evaluates the real part of the dot product of the Hermitian conjugate of one vector with a second vector. The weight is compared with the previous  $W_{pq}(\mathbf{R})$  and the move is accepted or rejected accordingly. If it is accepted, interpolation variables generated in INTERP are saved with the call SAVEIT. This procedure is repeated a number of times to obtain a statistically independent position. A final call to entry RESTOR makes sure the interpolation data for the last accepted move is available before returning to the main program.

The bulk of computation is in the construction of the wave function performed by WAV, given the particle positions and order of operators. WAV starts with the uncorrelated spin-isospin state  $\Phi$  and multiplies in the product over pairs of central correlations  $f^c$ . Then the product of correlation operators is built up by successive calls to subroutine F60P in the order specified. F60P takes an input wave function vector  $\Psi$  and functions  $c_k$  and returns the result  $O\Psi$  where  $O$  is the operator of (9.19). The subroutine uses the mathematics of (9.26–28) and is written in real arithmetic for speed. More than 50% of the entire code's floating-point operations are executed inside F60P. The  $c_k$  passed by WAV to F60P include both the non-central two-body correlations  $u^k$  and the central three-body correlation  $f_3$  of (9.20).

Once a new sample  $W_{pq}(\mathbf{R})$  has been found, the contribution to any desired expectation value can be calculated. The energy is calculated by subroutines EKIN, VPOT, and TBPO, which evaluate the kinetic, two-body potential, and three-body potential, respectively. Contributions to the density distribution are incremented with the subroutine RHOR. EKIN computes derivatives of  $\Psi(\mathbf{R})$  by differences, as in (9.31), by repeated calls to INTERP and WAV (and F60P). After a call to subroutine INTRPV to obtain interpolated potential functions, VPOT evaluates the first six operator terms in the potential by another call to F60P. Spin-orbit terms in the potential are evaluated with the aid of gradients generated and stored by EKIN. Finally the Coulomb potential is evaluated with the charge operator  $(1 + \tau_{zi})(1 + \tau_{zj})e^2/r_{ij}$ . (A charge form factor is included in our routine.) TBPO loops over all triples to evaluate the three-body potential contributions. It makes use of two subroutines, STONE and STAC, which have logic very similar to F60P, but

are specialized for the pair operators in the three-nucleon interaction. The three-body force may be written in a form involving the commutators and anticommutators of these pair terms, which are evaluated in the routine STAC.

A running sum is kept of the various components of the energy and of their squares for the calculation of the variance. If an energy difference with a different wave function is being computed, terms for the covariance are also kept. After a certain number of energies are evaluated, a local average and variance (and difference with its variance if appropriate) are computed and printed out, along with a running global average and variance. When the desired total number of configurations have been evaluated, the counters for the density distribution are processed, and the rms radius for protons and neutrons is calculated, and these items are also printed out. The program ends with a printout of the total execution time, number of floating-point operations, which have been tracked with counters in the subroutines, and resulting speed for the code.

The code can be generalized to handle other Hamiltonians, and the wave function can be used to compute other expectation values. The code has been written for execution on a vector processor, but many of the tricks used are also valuable on scalar machines. For nested DO loops, the longest possible ones are placed innermost, and where possible, run over multiple indices. For example, loops over both spin and isospin indices frequently run over IJ=1, NS\*NT with functions dimensioned F(NS,NT) indexed as F(IJ,1). (This has the disadvantage of giving error messages if a bounds checker is used.) A number of further improvements can be made that will increase performance, but they have been omitted here for simplicity. Real arithmetic is generally faster than complex, and explicitly real versions of the subroutines STONE and STAC are useful. The kinetic-energy calculation can be sped up significantly on a vector processor by making versions of subroutines WAV and F6OP that compute the 6A wave functions needed for gradients at the same time, i.e., with the innermost DO loop running over an index L=1, 6\*NPART. Memory-bank conflicts can be reduced on some machines by adding one unit to the size of the leading dimension in many arrays, e.g., dimensioning objects like F(NS+1,NT). These are the primary differences between the code presented here and our regular production code.

## 9.7 Technical Note

The code is not intended to be run on a microcomputer. Thus we have not tried to convert it to strict ANSI-standard FORTRAN 77. For example, the program uses complex\*16 arithmetic which is not available in ANSI-standard FORTRAN 77 and will not be supported by a personal computer.

The diskette contains example input (VARMCH3.INP) and output (VARMCH3.OUT) files which both correspond to studies of the  $^3\text{H}$  nu-

cleus with the present program.

## 9.8 Acknowledgment

J. Carlson would like to thank the U. S. Department of Energy for its support of this work, and R. B. Wiringa would also like to thank the Nuclear Physics Division of the Department of Energy, contract W-31-109-ENG-38.

## References

- [9.1] J. Lomnitz Adler, V. R. Pandharipande, and R. A. Smith, Nucl. Phys. **A315** (1981) 399
- [9.2] J. Carlson, V. R. Pandharipande, and R. B. Wiringa, Nucl. Phys. **A401** (1983) 59
- [9.3] R. Schiavilla, V. R. Pandharipande, and R. B. Wiringa, Nucl. Phys. **A449** (1986) 219
- [9.4] R. B. Wiringa, to be published.
- [9.5] J. Carlson, J. Kogut, and V. R. Pandharipande, Phys. Rev. **D27** (1983) 233
- [9.6] J. Carlson, J. Kogut, and V. R. Pandharipande, Phys. Rev. **D28** (1983) 2807
- [9.7] J. Carlson, K. E. Schmidt, and M. H. Kalos, Phys. Rev. **C36** (1987) 27
- [9.8] S. Pieper, R. B. Wiringa, and V. R. Pandharipande, Phys. Rev. Lett. **64** (1990) 364
- [9.9] M. H. Kalos, Phys. Rev. **128** (1962) 1791
- [9.10] M. H. Kalos, D. Levesque, and L. Verlet, Phys. Rev. **A9** (1974) 2178
- [9.11] K. E. Schmidt, in *Models and Methods in Few-Body Physics*, Lecture Notes in Physics 273 (Springer, Berlin, Heidelberg, 1987)
- [9.12] P. J. Reynolds, D. M. Ceperley, B. J. Alder, and W. A. Lester, J. Chem. Phys. **77** (1982) 5593; D. M. Ceperley and B. J. Alder, J. Chem. Phys. **81** (1984) 5833
- [9.13] J. Carlson, Phys. Rev. **C38** (1988) 1879
- [9.14] J. Carlson, Phys. Rev. **C36** (1987) 2026
- [9.15] K. E. Schmidt and J. W. Moskowitz, J. Chem. Phys. **76** (1982) 1064
- [9.16] K. E. Schmidt, M. H. Kalos, M. A. Lee, and G. V. Chester, Phys. Rev. Lett. **45** (1980) 573
- [9.17] N. Metropolis, A. W. Rosenbluth, M. N. Rosenbluth, A. H. Teller, and E. Teller, J. Chem. Phys. **21** (1953) 1087
- [9.18] Malvin H. Kalos and Paula A. Whitlock, *Monte Carlo Methods*, Vol. I (Wiley, New York, 1986)
- [9.19] A. De Rújula, Howard Georgi, and S. L. Glashow, Phys. Rev. **D12** (1975) 147
- [9.20] R. B. Wiringa, R. A. Smith, and T. L. Ainsworth, Phys. Rev. **C29** (1984) 1207
- [9.21] M. Lacombe, B. Loiseau, J. M. Richard, R. Vinh Mau, J. Côté, P. Pirés, and R. de Tourreil, Phys. Rev. **C21** (1986) 861
- [9.22] M. M. Nagles, T. A. Rijken, and J. J. de Swart, Phys. Rev. **D17** (1978) 768
- [9.23] R. V. Reid, Ann. Phys. (N.Y.) **50** (1968) 411
- [9.24] S. A. Coon, M. D. Scadron, P. C. McNamee, B. R. Barrett, D. W. E. Blatt, and B. H. J. McKellar, Nucl. Phys. **A317** (1979) 242
- [9.25] I. E. Lagaris and V. R. Pandharipande, Nucl. Phys. **A359** (1981) 349

- [9.26] R. Schiavilla, A. Fabrocini, and V. R. Pandharipande, Nucl. Phys. **A473** (1987) 290
- [9.27] R. Schiavilla, V. R. Pandharipande, and D. O. Riska, Phys. Rev. **C41** (1990) 309
- [9.28] R. Schiavilla, et al., Nucl. Phys. **A473** (1987) 267